Macroelement and Macropatch Approaches to Structural Topology Optimization Using the Ground Structure Method

Xiaojia Zhang, S.M.ASCE[1]; Sushant Maheshwari[2]; Adeildo S. Ramos Jr.[3]; and Glaucio H. Paulino, M.ASCE[4]

Abstract: Topology optimization can be divided into continuum and discrete types, the latter being the emphasis of the present work. In the field of discrete structural topology optimization of trusses, the generation of an initial ground structure is crucial. Thus, this paper examines the generation of ground structures for generic structural domains in two and three dimensions. It compares two methods of discretization, Voronoi-based and structured quadrilateral discretizations, and proposes two simple and effective ground structure generation approaches: the macroelement and macropatch approaches. Both can be implemented with either type of discretization. This work presents several features of these approaches, including the efficient generation of initial ground structures, a reduction in matrix bandwidth for the global stiffness matrix, finer control of bar connectivity, and a reduction in the number of overlapped bars. Generic examples and practical structural engineering designs are presented. They display the features of the proposed approaches and highlight the comparison with results from either the literature, the traditional ground structure generation, or the continuum optimization method.
DOI: 10.1061/(ASCE)ST.1943-541X.0001524.

Author keywords: Truss layout optimization; Ground structure method; Voronoi-based mesh; Macroelement approach; Macropatch approach; Structural optimization.

Introduction

In an effort to attain structural efficiency, a promising technique used for optimizing the truss layout is the ground structure method (GSM) (Dorn et al. 1964; Christensen and Klarbring 2008; Bendsøe and Sigmund 2003). This method can be used to study the flow of forces within a domain, and to obtain the optimal design of structures. The generation of the initial ground structure is a crucial aspect of the GSM. For example, Smith (1998) proposed an approach that employs unstructured grids to represent the design domain; however, the approach requires additional preprocessing steps, including the decomposition of design elements and the generation of boundary faces. Other studies (Rule 1994; McKeown 1998; Martinez et al. 2007; Hagishita and Ohsaki 2009) proposed growing methods that tend to use a small size of the initial ground structure, but the size of the structure later needs to be expanded during the optimization. Furthermore, the use of various connectivity levels have been investigated by a number of studies (e.g., Ben-Tal and Bendsøe 1993; Bendsøe et al. 1994; Bendsøe and Sigmund 2003; Achtziger and Stolpe 2007; Sokół 2010), showing that different initial ground structures may result in different final topologies. A well-known problem with the leveling method is that the assignment of a sufficient connectivity level is problem-dependent. Hence, the main purpose of this paper is to propose new approaches to generate ground structures and to improve the results of the traditional GSM.

One limitation associated with the traditional GSM is the generation of invalid connectivity. For concave domains (Ω), as illustrated in Fig. 1(a), or distinct design domains (Ω_1 and Ω_2), as illustrated in Fig. 1(b), it is necessary to verify that connections do not fall outside the boundary of concave domains or cross the border of distinct design domains. With the approaches presented in the present paper, these problems are circumvented.

In this paper, the proposed approaches are compared with the full-level classical GSM. In the GSM, a set of nodes discretizes the domain, and then the nodes are connected by truss members. For a full-level ground structure, all nodes in the domain are connected, giving a fully populated global stiffness matrix that adds to the computational cost (Heath 1997). In an effort to reduce the computational cost, a number of studies have defined various connectivity levels (Sokół 2010), whose underlying concept is that the final topology does not require long bars. Thus, many bars in full-level ground structures are unused in the optimization process (Gilbert and Tyas 2003). In addition, the use of lower levels of connectivity may reduce the computational cost associated with these unused bars in the optimization process. However, it is impractical to define a general ground structure level for all problems. Different connectivity levels may result in different topologies for the same problem, as illustrated in Fig. 2, in which the final topology of a

[1]Graduate Student, School of Civil and Environmental Engineering, Georgia Institute of Technology, 790 Atlantic Dr. NW, Atlanta, GA 30318. E-mail: xzhang645@gatech.edu

[2]Structural Engineer, Skidmore, Owings and Merrill LLP, 224 S. Michigan Ave., Suite 1000, Chicago, IL 60604. E-mail: sushant.maheshwari@som.com

[3]Associate Professor, Laboratory of Scientific Computing and Visualization Technology Center, Federal Univ. of Alagoas, Maceió, AL 57092-970, Brazil. E-mail: adramos@lccv.ufal.br

[4]Raymond Allen Jones Chair of Engineering, School of Civil and Environmental Engineering, Georgia Institute of Technology, 790 Atlantic Dr. NW, Atlanta, GA 30318 (corresponding author). E-mail: glaucio.paulino@ce.gatech.edu

Note. This manuscript was submitted on November 10, 2014; approved on February 1, 2016; published online on May 19, 2016. Discussion period open until October 19, 2016; separate discussions must be submitted for individual papers. This paper is part of the ***Journal of Structural Engineering***, © ASCE, ISSN 0733-9445.

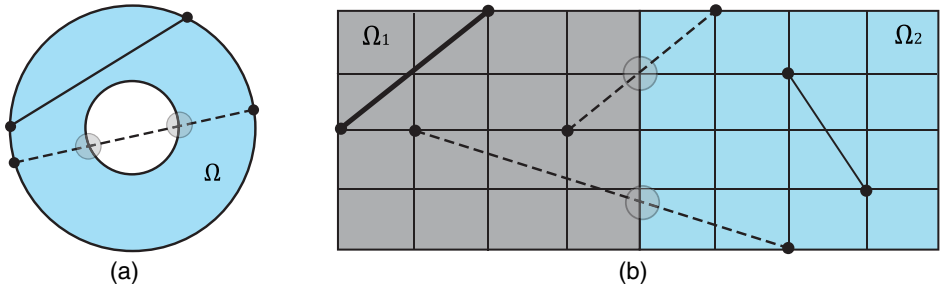

Fig. 1. Illustration of ground structure generation, in which the solid lines denote allowed connections and the dashed lines denote violated connections: (a) concave domain; (b) convex domain decomposed into two separate design regions

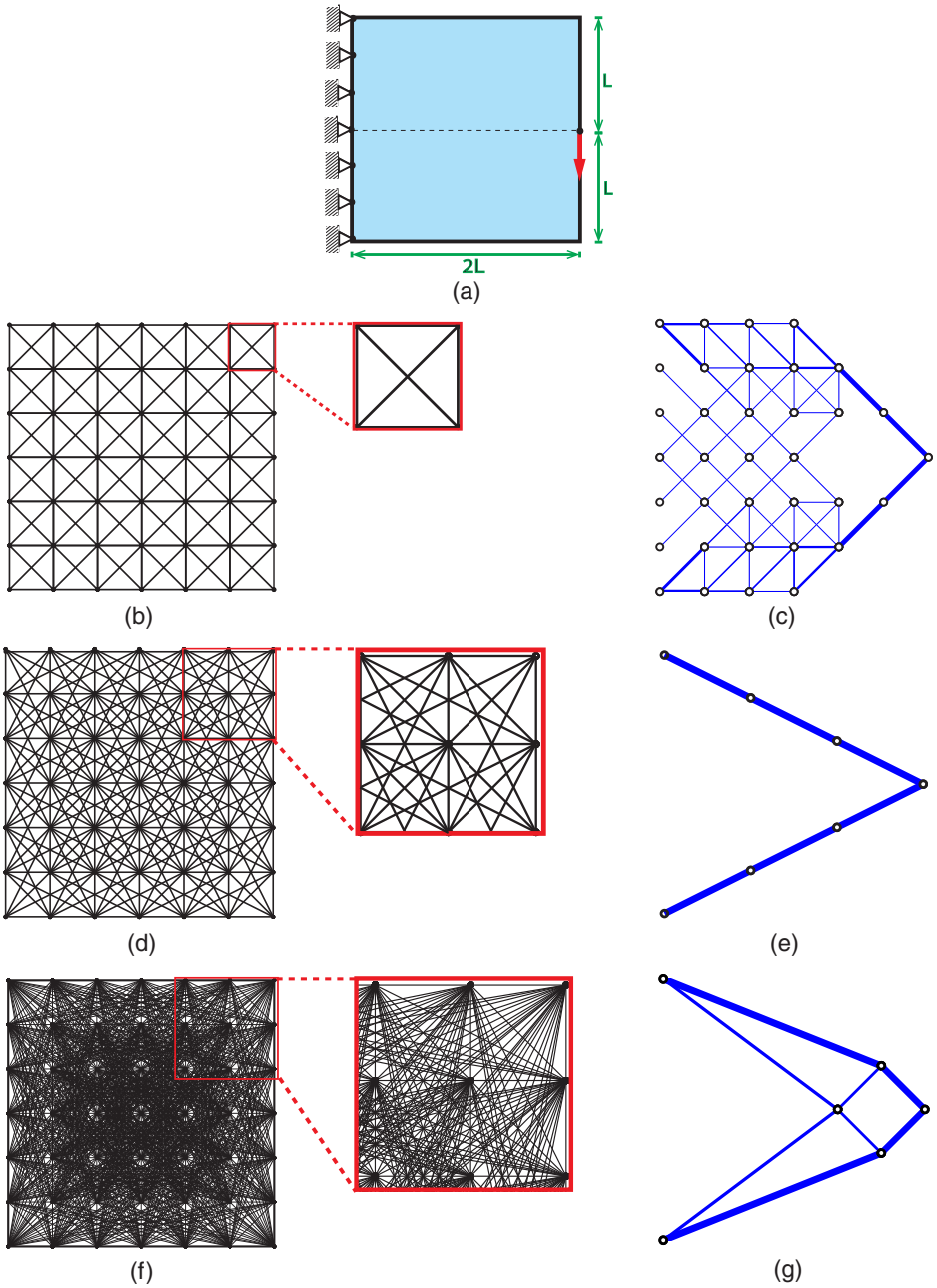

Fig. 2. Generation of the initial ground structure for three levels of connectivities: (a) box domain and boundary conditions; (b) level 1 ground structure; (c) level 1 optimal topology with normalized compliance $C = 1.58$; (d) level 2 ground structure; (e) level 2 optimal topology with normalized compliance $C = 1.02$; (f) full-level ground structure; (g) full-level optimal topology with normalized compliance $C = 1.00$

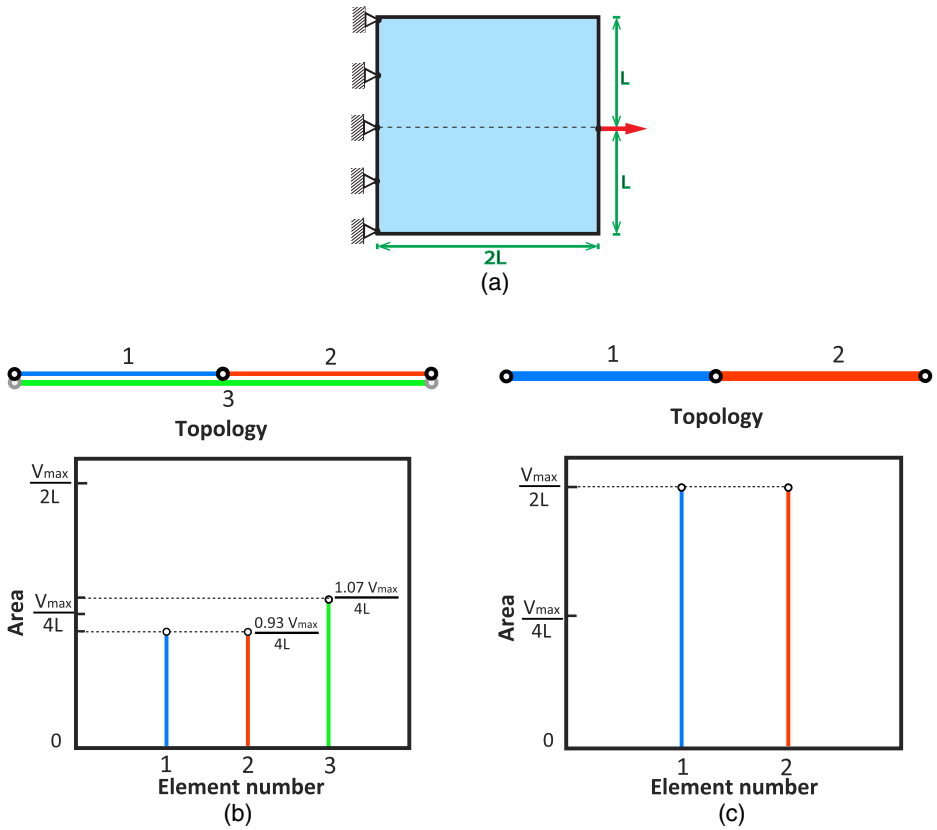

Fig. 3. Topology optimization with and without overlapping bars in a box domain (discretized by a 2×2 grid): (a) box domain and boundary conditions; (b) optimal topology and bar area plot with overlapping bars; (c) optimal topology and bar area plot with nonoverlapping bars

level 2 ground structure in Fig. 2(e) has a simple design, whereas the topology of a full-level ground structure in Fig. 2(g) provides the best solution in terms of compliance. This work analyzes only full-level ground structures with the classic GSM.

In the GSM, overlapping bars are undesirable in the initial ground structure when issues of stability and buckling are not considered. The bars can be removed either during or after the member-generation process. As shown in Fig. 3, a simple example highlights the importance of removing overlapping bars. The solution of this problem is trivial: One straight horizontal member carries all of the load to the supports. (The issue of stability is beyond the scope of this work.) When the overlapping bars are not removed, the bar areas are not equal, as shown in Fig. 3(b). However, when the overlapping bars are removed, all of the bar areas are equal [Fig. 3(c)]; the sum of bar areas (at a location of the bar) of the overlapping case is equal to the corresponding bar area of the nonoverlapping case. Thus, to obtain meaningful and practical results, even in the simplest examples, one should remove overlapping members. In addition, the removal of the overlapping bars reduces the total number of bars in the model and decreases the computational cost. In this work, the authors remove overlapping bars during the member-generation process.

Under equal stress limits, for a structure to be optimal, all members should be fully stressed (Michell 1904), leading to the requirement that all tensile and compressive bar pairs should intersect orthogonally (for problems without material or geometric nonlinearities). Therefore, if all bars are assumed to have the same stress limits, orthogonality in pairs of bars should appear in optimal configuration patterns (Ohsaki 2010). The Michell's discrete solution (Michell 1904; Sokół and Rozvany 2012) typically has infinitely dense members. Employing the traditional GSM, the authors approximate the theoretical solution by using a finite number of structural members extracted from the original ground structure.

This paper proposes two simple and effective approaches to generate initial ground structures, the macroelement and macropatch approaches, which are capable of generating initial ground structures for design domains of nontrivial geometries with ease, and do not require any additional information about the outer and inner boundaries of the domain. The two approaches, proposed in a general setting, may be combined with any type of discretization, including quadrilateral and Voronoi-based grids, in two or three dimensions. Furthermore, the two approaches can be implemented in both elastic and plastic formulations. The elastic formulation is adopted in this paper (Christensen and Klarbring 2008; Bendsøe and Sigmund 2003), because it can be easily extended to a wider class of problems, such as material and geometrical nonlinearity and multiple load cases, which is not the case for the plastic formulation.

In this paper, the authors optimize truss layouts to approximate available analytical solutions, to study the force flow of non-box (concave) domains, and most importantly, to obtain a practical design of structures. One focus of this paper is to approximate the discretized Michell truss and optimize a nonbox domain to verify the solutions obtained using new approaches with the analytical solution, and demonstrate the capabilities of the proposed approaches with respect to different geometries. Another focus is the optimization of structural engineering problems, including a skyscraper and a long-span bridge. General examples and structural engineering designs are presented that highlight the features of the proposed approaches and compare the results from the literature, the traditional GSM, and the continuum optimization method.

This paper is organized as follows: First is a review of the ground structure optimization formulation for compliance minimization,

using only the cross-sectional areas of the bars as the design variables. Next is an introduction to discretization methods and the proposed macroelement and macropatch approaches, with a discussion of their attributes for the optimization of trusses using the GSM. Finally, several numerical examples highlight the properties of the new approaches, and some concluding remarks provide suggestions for extending the work.

Problem Formulation

Optimization Formulation

In this work, equilibrium, compatibility, and constitutive relations are taken into account, which are explicitly known as the elastic formulation (Kirsch 1989). The authors assume that the initial ground structure has N nodes and M members. The equilibrium state of the system can be described by

$$\boldsymbol{K}\boldsymbol{u} = \boldsymbol{f} \tag{1}$$

where for the case of a two-dimensional (2D) problem, $\boldsymbol{f} \in R^{2N}$ = external force vector; $\boldsymbol{u} \in R^{2N}$ = displacement vector; and $\boldsymbol{K} \in R^{2N*2N}$ = stiffness matrix. For a full-level ground structure in a convex domain before removing the overlapping bars, the relation between M and N is $M = N(N-1)/2$.

The stiffness matrix $\boldsymbol{K}$ can be expressed as (Christensen and Klarbring 2008)

$$\boldsymbol{K}(\boldsymbol{a}) = \sum_{i=1}^{M} a_i \boldsymbol{K}_i^0, \qquad \boldsymbol{K}_i^0 = \frac{E_i}{\ell_i}\boldsymbol{b}_i\boldsymbol{b}_i^T \tag{2}$$

where $\boldsymbol{K}_i^0$ = constant matrix in global coordinates associated with each member; E_i = Young's Modulus; and ℓ_i = length of member i. Moreover, $\boldsymbol{a} \in R^M$ = vector of the design variables (areas of bars) for the optimization problem; and $\boldsymbol{b_i}$ = vector describing the orientation of member i of the form

$$\boldsymbol{b_i} = \{\cdots \; -\boldsymbol{n}^{(i)} \; \cdots \; \boldsymbol{n}^{(i)} \; \cdots\}^T \tag{3}$$

where $\boldsymbol{n}^{(i)}$ = unit vector in the axial direction of member i.

Here, the optimization problem is defined as obtaining a set of design variables that minimizes the compliance of the structure subjected to equilibrium and volume constraints. Because the main purpose of this paper is to explore the connectivity generation in the initial ground structure, the authors adopt the simplest displacement-based formulation with a small positive lower bound imposed on the design variables a_i. The nested formulation has been shown to be convex (Svanberg 1984). The problem statement with multiple load cases is formulated as (Bendsøe and Sigmund 2003)

$$C(\boldsymbol{a}) = \min_{\boldsymbol{a}} \sum_{j=1}^{q} \alpha_j \boldsymbol{f}_j^T \boldsymbol{u}_j(\boldsymbol{a}),$$
$$\text{s.t.} \begin{cases} g(\boldsymbol{a}) = \boldsymbol{a}^T\boldsymbol{L} - V_{\max} \le 0, \\ a_i^{\min} \le a_i \le a_i^{\max} \quad \forall\ i = 1{:}M \end{cases} \tag{4}$$

where $\boldsymbol{u}_j$ = solution of Eq. (1); $C(\boldsymbol{a})$ = objective function; q = number of load cases; α_j = weighting factor of load case j; $g(\boldsymbol{a})$ = constraint function; $\boldsymbol{a}$ and $\boldsymbol{L}$ = vectors of area and length, respectively; $V_{\max}$ = maximum material volume; and $a_i^{\max}$ and $a_i^{\min}$ = upper and lower bounds, respectively.

This formulation allows the efficient computation of the element stiffness matrices. The global stiffness matrix can then be assembled from element stiffness matrices and current design variables (i.e., member cross-sectional areas). This feature facilitates the development of an efficient computational implementation. To avoid a singular stiffness matrix in the solution of Eq. (1), zero member areas are avoided by a small lower bound, $a_i^{\min}$. An upper bound, $a_i^{\max}$, is also imposed to ensure robustness of the formulation. Throughout this work, the lower and upper bounds are defined by $a_i^{\min} = 10^{-2}a_0$ and $a_i^{\max} = 10^3 a_0$, respectively, in which a_0 is the average area defined as

$$a_0 = V_{\max} \Big/ \sum_i L_i \tag{5}$$

Implementation Aspects

The concepts in this paper were implemented in a complete truss layout optimization solver in *MATLAB*. The implementation consists of two components: initial ground structure generation and optimization. The initial ground structure generation process includes the initial grid generation and connectivity generation. To generate the initial grid of a domain, three alternatives are employed: the generation of Voronoi-based grids using the mesh generator for polygonal elements, PolyMesher (Talischi et al. 2012a); the generation of structured quadrilateral grids using an intrinsic subroutine; or importing unstructured grids from elsewhere. Here, the main idea of the initial ground structure generation is to produce nonoverlapping connectivity using the initial grid. Testing for mutually overlapped connections is an additional procedure that is used to generate connectivity in the traditional GSM. The optimization process contains three components: solving the structural equilibrium problem for a set of given design variables, computing the sensitivities of the design variables, and updating design variables based on the optimality criteria (OC). Details of the OC are provided in the Appendix.

Ground Structure Generation

Initial Grid

In this paper, two types of grids are used to discretize the domain: structured quadrilateral and Voronoi-based grids, as shown in Fig. 4. The use of a specific grid type is problem-dependent. Indeed, points can be distributed without an initial grid and provide a good basis for a ground structure, but this is true under the condition that the points are distributed uniformly in the domain, whereas the use of the initial grid readily provides a set of evenly distributed nodes in the domain. Moreover, the distribution of the nodes can be controlled by the element quality in the grid.

The use of a structured quadrilateral grid in a full-level ground structure provides pairs of orthogonal bars by construction, but the truss members tend to orient in a limited number of directions. In addition, when the domain is nonconvex, the procedure for generating grids is generally tedious, as the restriction zones need to be identified (Zegard and Paulino 2014).

As an alternative, the use of the Voronoi-based grid is proposed. Voronoi-based grids easily discretize nonconvex domains and have been shown to be advantageous in continuum topology optimization (Talischi et al. 2009, 2010, 2012a, b). The seeds of Voronoi-based grids are initially generated randomly, then iterated to align more uniformly to form a centroid Voronoi tessellation (CVT). After extracting the node and element information, the optimization procedure is the same as for structured quadrilateral or other discrete grids. Voronoi-based discretization, as compared with the structured quadrilateral one, has a greater possibility of

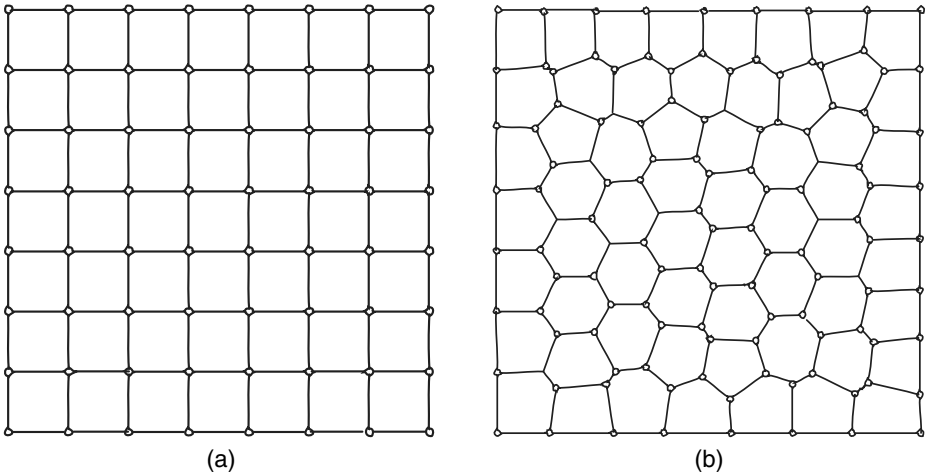

Fig. 4. Discretization techniques for forming the base grid: (a) structured quadrilateral grid; (b) Voronoi-based grid

providing truss members with various directions because of its initial random node distribution. When the domain is concave or contains holes, the Voronoi-based grid is the preferred discretization in this work. For these domains, as the generated bars have to be entirely within the domain, not all connections are feasible. Therefore, additional information on the outer and inner boundaries of the domain is needed with respect to the traditional GSM. This issue is naturally solved by the member generation approaches that are proposed, which is further discussed in section "Attributes and Properties."

Member Generation Approaches

In this section, two approaches for generating the initial ground structures using structured quadrilateral and Voronoi-based grids in two or three-dimensional domains are presented. A macroelement approach and a macropatch approach are proposed to overcome some of the difficulties in generating the initial ground structure that are discussed previously.

Macroelement Approach

The basic idea behind this method is to insert equally spaced nodes on each edge of each element, then connections are only generated within each element. The macroelement approach is illustrated in Fig. 5. Different scenarios are considered to show the flexibility of this method: Three equally spaced nodes are inserted on each edge for the structured quadrilateral element in Figs. 5(a–c), and one node is inserted per edge for the wrench domain with the Voronoi-based grid in Figs. 5(d–f).

Macropatch Approach

Generating the initial ground structure for three-dimensional (3D) curved surfaces is a challenge that can be overcome by assuming that the curved surface is a collection of different facets or patches. For a curved surface, the patches cannot be guaranteed to be in the same plane; thus, patch connectivity is done individually for each patch. Determining the size of the patch is usually based on the computational time and the level of detail that the user wants. In the current paper, only structured grids are used in the macropatch approach; however, this approach can be extended to Voronoi-based grids as well.

Each patch is represented as a unit. Additional bars and nodes are created by dividing the macropatch into subpatches; the total resulting nodes within the original patch are then interconnected to each other. An illustration of a single element and a tower domain in 3D is shown in Fig. 6.

Attributes and Properties

The properties of the macroelement approach and the macropatch approach relate to the initial ground structure generation process, optimization process, and final topology. In the initial ground structure generation process, the proposed approaches avoid invalid connections outside the boundary (for concave domains) by construction, as illustrated in Fig. 7(a). For the case of concave domains, the initial ground structure can be generated efficiently as long as the domain is discretized and the member connectivity matrix is known. These approaches can also be used to prevent connections across separated design domains, Ω_1 and Ω_2, as shown in Fig. 7(b). Thus, the bars can be generated without the additional step of detecting boundaries or checking for feasible connections.

Another attribute of the two approaches relates to the optimization process. The global stiffness matrices generated using the two new approaches have reduced maximum semi-bandwidths. This advantage becomes important when the problem size is large. After the nodes have been inserted on the edge of each element, the reverse Cuthill–McKee (RCM) algorithm (Cuthill and McKee 1969) is applied to renumber the nodes. Because bars are only generated in each element, the maximum semibandwidth for the global stiffness matrix of the problem will be reduced accordingly.

In terms of the final topology, the macroelement and macropatch approaches offer alternative bar distributions for a similar number of design variables by providing finer control of the connectivity. Different types of connectivity can be achieved by changing the number of nodes inserted on the edge. Although the classic GSM can be created such that it encompasses the proposed approaches, this is at the expense of using a much denser ground structure and a much greater number of design variables. In addition, either curved or straight paths can be achieved with the proposed approaches and the classic GSM. If an overall curved path is desired, the node distribution needs to be dense enough for the classic GSM to obtain an overall curved path. However, the proposed approaches are capable of generating an overall curved path with a coarse grid, as shown in Fig. 8(b). Section "Examples and Verification" further demonstrates this feature.

Furthermore, the two proposed methods generate much less overlapping bars in the domain. For the macroelement approach, overlapping bars appear only on the (refined) element boundary, and can be efficiently and systematically removed. For the macropatch

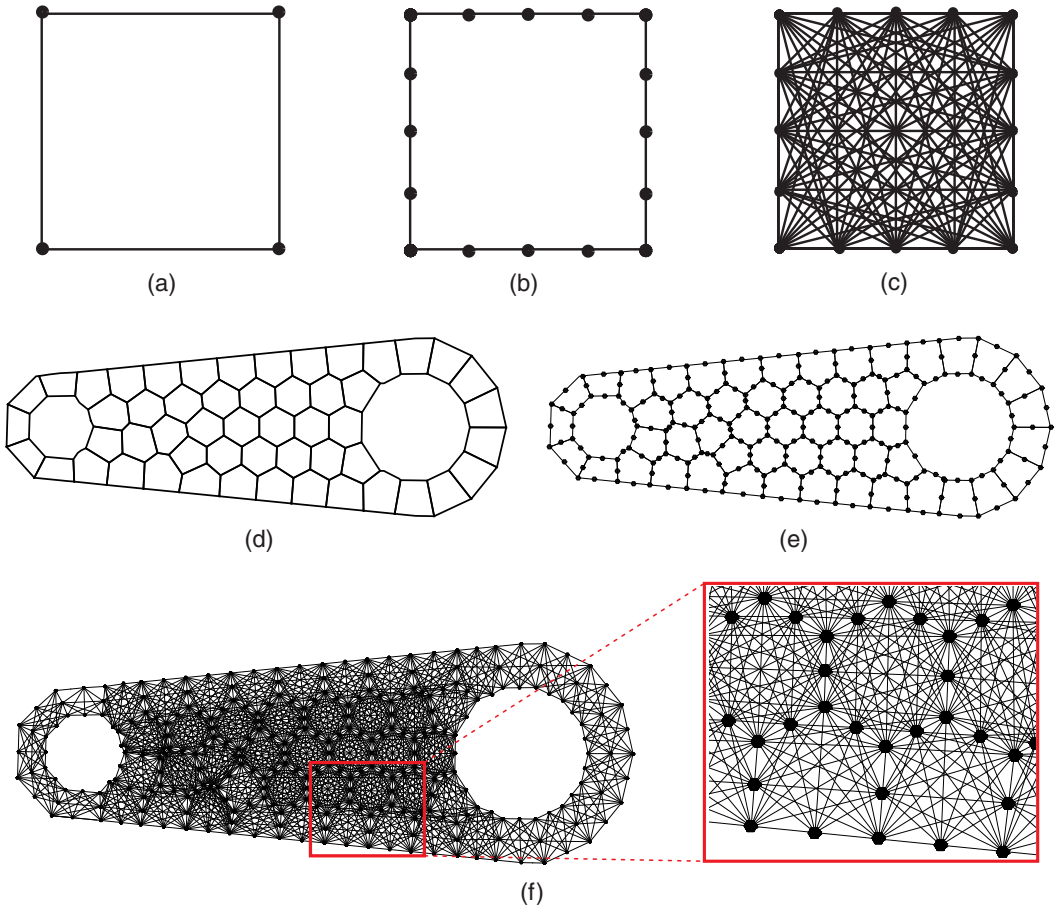

Fig. 5. Macroelement approach: (a) standard single-structured quadrilateral element; (b) single element with three nodes inserted on each edge; (c) all possible connections within the element; (d) wrench domain with a Voronoi-based grid; (e) wrench domain with one node inserted on each edge; (f) all possible connections within each element

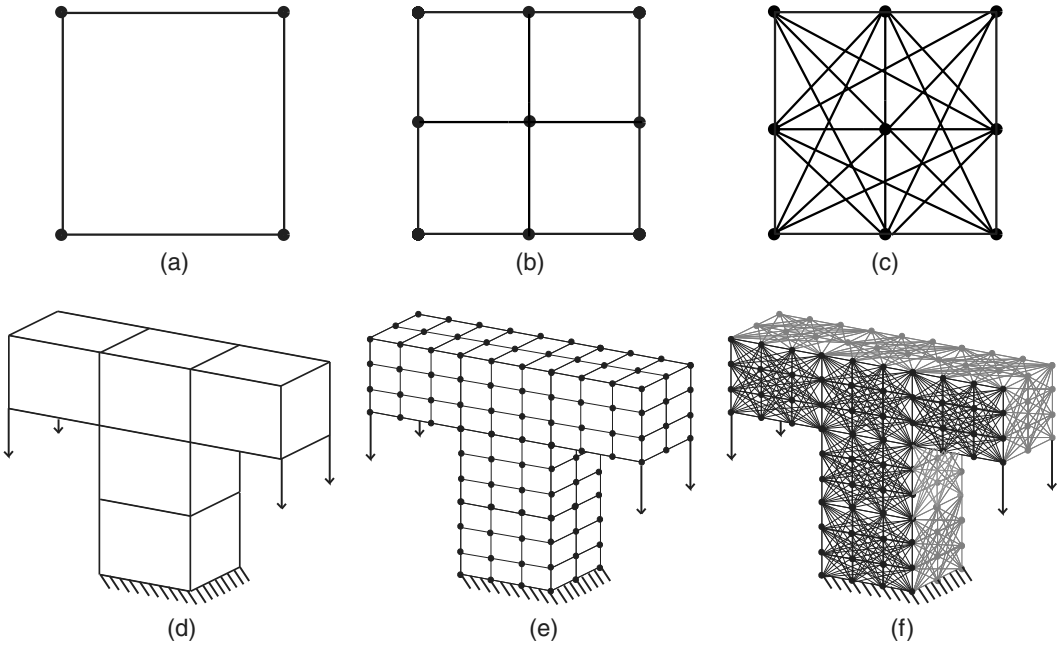

Fig. 6. Macropatch approach: (a) single-structured quadrilateral patch; (b) single patch divided into 2×2 subpatches; (c) all possible connections within the patch; (d) 3D tower domain and boundary conditions; (e) 3×3 subpatches on front-surface elements, and 3×2 subpatches for side-surface elements; (f) all connections within each patch surface

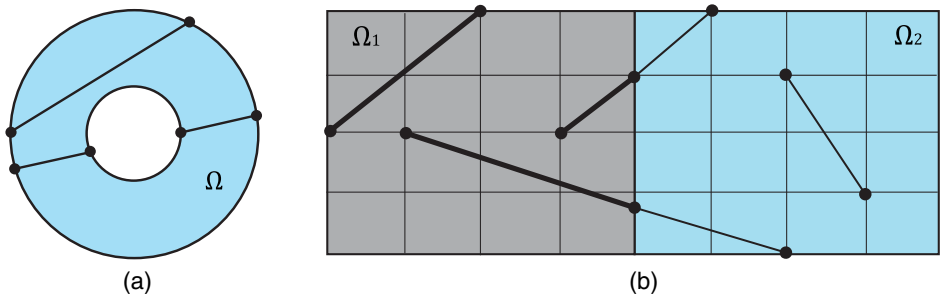

Fig. 7. Optimization problems using macroelement approach and macropatch approach to correctly generate initial ground structures with valid connections: (a) concave domain; (b) convex domain with separated design domains

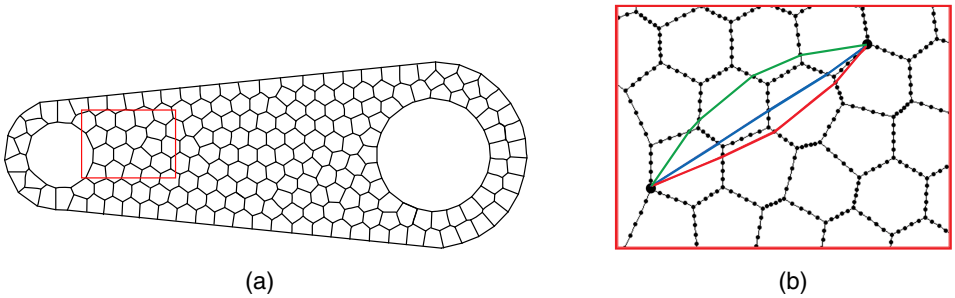

Fig. 8. (a) Wrench domain with a boxed zoom-in region; (b) possible connectivity using the macroelement approach

approach, even though removing overlapping bars is still an issue, the problem of finding and removing these bars becomes a reduced local problem with a lower associated computational cost.

The two proposed approaches are general enough to be used with any type of discretizations, including the structured quadrilateral and Voronoi-based grids. These techniques can handle different types of domains, concave or convex, and in two or three dimensions. In addition, because the macroelement approach and macropatch approach are independent of the optimization formulations, they are flexible and can be extended to other applications with ease.

Examples and Verification

Three types of problems are studied in this paper to demonstrate the various features of the proposed approaches:

- Benchmark example: Michell truss;
- Nonbox (concave) domain: wrench; and
- Structural engineering applications: long-span bridge, skyscraper.

The Michell truss example is used to verify solutions of the new approaches with a benchmark problem with an available analytical solution. The example with a nonbox (concave) domain is used to demonstrate the capability of the new approaches and to study the force flow in the design phases. The third type of example is the optimization of structures with engineering applications to showcase the use of the new approaches in structural designs. The first three examples use the macroelement approach with Voronoi-based and quadrilateral grids, including comparisons with the traditional GSM and continuum optimization method, and the last example uses the macropatch approach on a structured quadrilateral grid in a 3D shell configuration.

All examples are performed with the same volume constraint, $V_{\max} = A_\Omega \times t$, in which A_Ω is the area of the domain; the stopping criterion is chosen as $\text{tol} = 10^{-8}$; the move value as $\text{move} = (a_i^{\max} - a_i^{\min}) \times 100$; and the damping factor for the OC update scheme as $\eta = 0.7$ (Appendix). The Young's modulus for all of the bars is taken to be $E_0 = 2 \times 10^8$, the load vector is $\boldsymbol{f_i} = 1$ for point load, $\Sigma \boldsymbol{f_i} = 1$ for distributed load, and the initial guess of bar areas is chosen as $a_{\text{initial}} = 0.7 \times a_0$. The examples aim to demonstrate the proposed approaches. Choosing the cut-off value to define the final topology is a common problem in the ground structure method; bars with normalized areas above the cut-off value are plotted. The cut-off value is problem-dependent. For the Michell truss and the wrench examples, the cut-off value is 0.001. For the bridge and the tower examples, the cut-off values are 0.01 and 0.15, respectively. A larger cut-off value tends to exclude structurally important bars on the final topology, whereas a smaller cut-off value results in plotting many small area bars (Christensen and Klarbring 2008).

Comparison with Analytical Solution

The main objective of this example is to compare results from the traditional GSM and the macroelement approach in approximating the Michell's solution of a simply supported beam, as shown in Fig. 9(a). For the Michell's analytical solution, readers are referred to Michell (1904) and Sokół and Rozvany (2012). Both structured quadrilateral and Voronoi-based discretizations are used in the box domain with the traditional GSM and the macroelement approach. Key features of the results are presented in Table 1.

The final topologies, using the full-level traditional GSM with a structured quadrilateral grid and a Voronoi-based grid, are

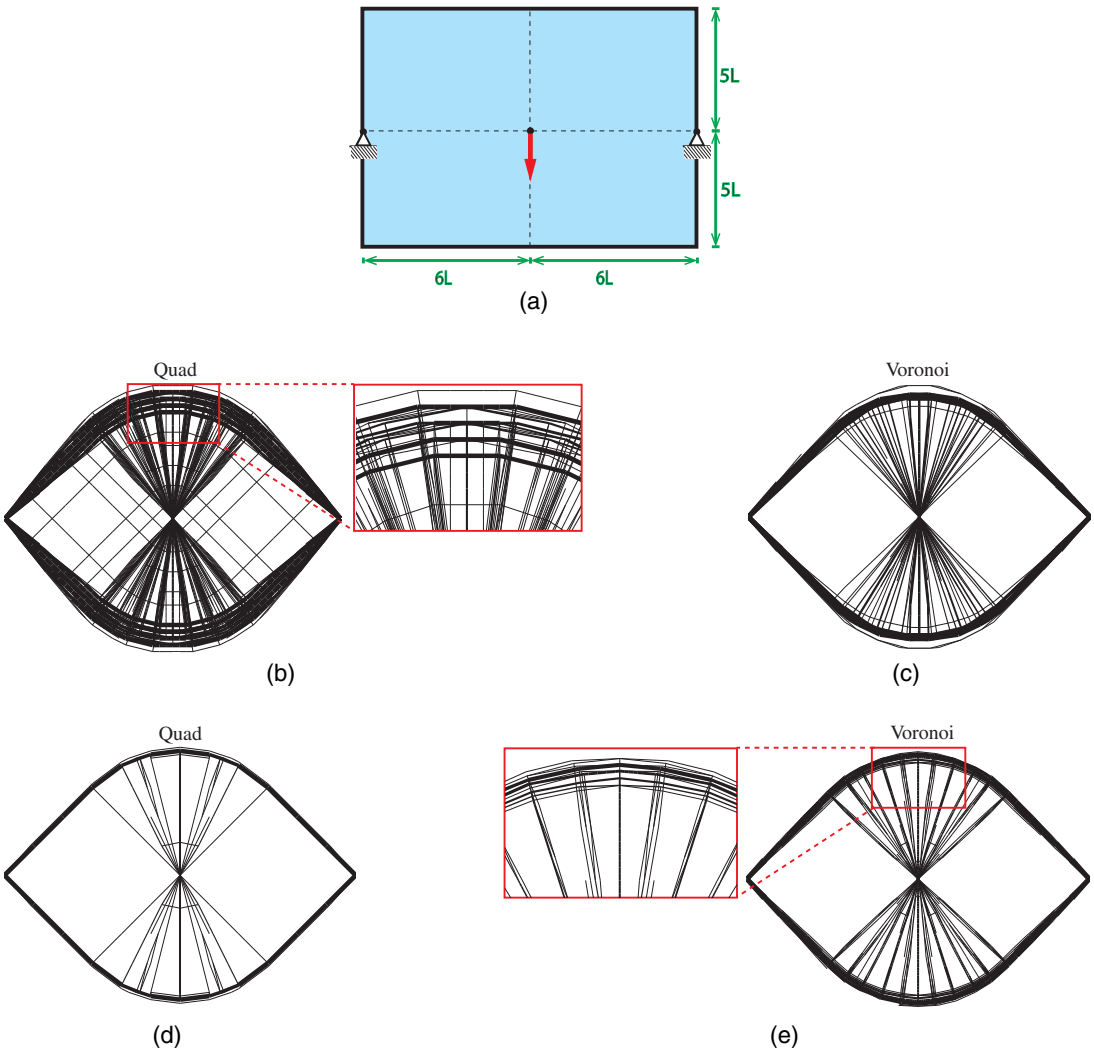

Fig. 9. Approximation of Michell's solution in a box domain using both a structured quadrilateral grid and a Voronoi-based grid: (a) box domain with boundary conditions; (b) topology obtained from the traditional GSM with a structured quadrilateral grid with 1,080 elements; (c) topology obtained from the traditional GSM using a Voronoi-based grid with 800 elements; (d) topology obtained from the macroelement approach using a structured quadrilateral grid of 120 elements with seven nodes inserted along each edge; (e) topology obtained from the macroelement approach using a Voronoi-based grid of 240 Voronoi-based elements with seven nodes inserted along each edge

Table 1. Numerical Information for Michell Truss Example

Grid	GSM	Number of bars	Number of DOFs	Compliance
Quadrilateral grid [Figs. 9(b and d)]	Traditional	77,710	2,294	1.7095
	Macroelement	59,520	3,954	1.6800
Voronoi-based grid [Figs. 9(c and e)]	Traditional	135,280	3,098	1.7099
	Macroelement	192,272	10,626	1.7049

illustrated in Figs. 9(b and c), respectively. The final topologies from the dense discretizations are similar to the analytical solution, but contain multiple layers along the boundary lines. By using the proposed macroelement approach, the topologies converge to the analytical solution, as shown in Figs. 9(d and e), for the structured quadrilateral and Voronoi-based grids, respectively. Because the Michell's analytical solutions typically consist of orthogonal and curved bars, the traditional GSM may not be able to approximate a curved path unless a very dense grid is used. However, in using the macroelement approach, the curved feature of the analytical solution is better approximated.

Application to Nonbox (Concave) Domain

The second example uses the macroelement approach for the wrench domain that was introduced in Talischi et al. (2012a). The nonbox domain is used to showcase the capability of the macroelement approach. The final topology is compared with that obtained using the traditional GSM.

Wrench Example: Comparison with Traditional GSM

This example considers the wrench domain with a Voronoi-based discretization, as shown in Fig. 10. The idea is to compare the final topology and the number of bars that are produced by both methods at a similar computational cost. In the traditional GSM, a Voronoi-based grid with 1,000 elements is used to discretize the domain, as illustrated in Fig. 10(b), with a full-level connectivity generated within the domain. Overlapping bars are removed during the bar-generating process. The final topology is shown in Fig. 10(d).

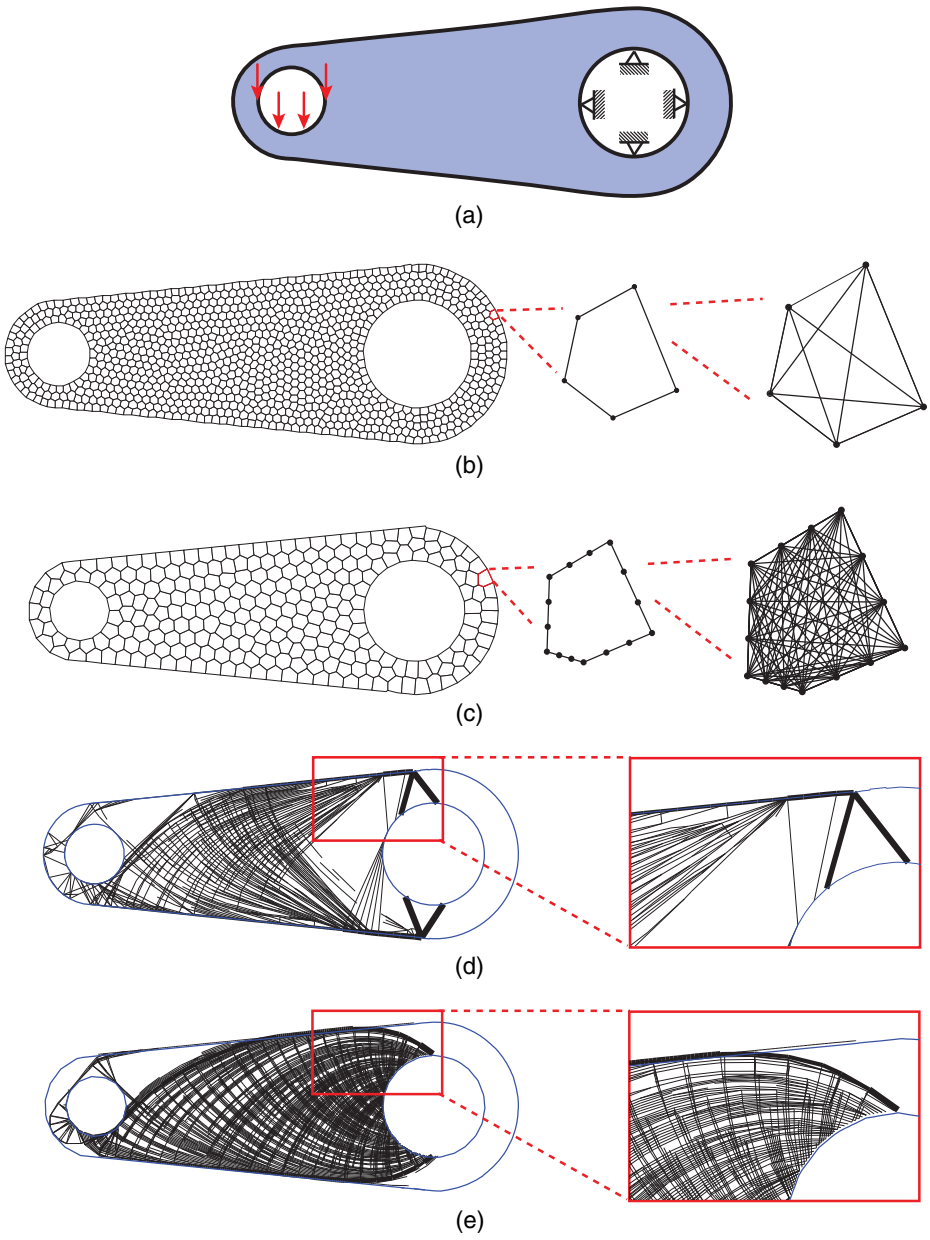

Fig. 10. Wrench example with Voronoi-based grid using classic GSM and macroelement approach: (a) wrench domain, maximum length: 2.8, maximum width: 1; (b) discretization using a Voronoi-based grid of 1,000 elements; (c) discretization using a Voronoi-based grid of 260 elements with seven additional nodes inserted along each edge (for clarity, the insert on the figure shows only two additional nodes along each edge); (d) final topology using the full-level classic GSM; (e) final topology using the macroelement approach

The boundary lines around the right-hand-side hole in the final topology are not smooth, and the bars in the middle of the domain are not detailed. The initial grid used in the macroelement approach is shown in Fig. 10(c), discretized by a Voronoi-based grid with 260 elements and seven additional nodes inserted along each edge. The final topology using the macroelement approach is shown in Fig. 10(e). Qualitatively, the macroelement approach results in a clear and crisp solution around the right-hand-side hole, and the bars inside the domain are smoother than those obtained using traditional GSM. In addition, the solution obtained using the macroelement approach exhibits the close-to-orthogonal pairs of bars.

A comparison of the number of bars, the number of degree of freedoms (DOFs) in the initial ground structures, and the final compliance values between the traditional GSM and the macroelement approach are presented in Table 2. This showcases the ability of the macroelement approach to handle the case of concave domains. In addition, the bar-generation process is efficient in the macroelement approach, because there is no need to detect the boundary or search for a large number of overlapping bars.

The source of the efficiency of the macroelement approach is apparent through a comparison of the maximum semibandwidth and profile of the stiffness matrix for both methods. The normalized maximum semibandwidth is computed as Max.semibandwidth/$2N$, and the normalized profile is computed as Profile/$[N(2N+2)+1]$, in which N is the number of nodes (Cook et al. 2002).

Both the maximum semibandwidth and the profile of the global stiffness matrices are significantly reduced when the macroelement

Table 2. Numerical Information for Wrench Example

GSM	Number of bars	Number of DOFs	Compliance	Normalized maximum semibandwidth	Normalized profile
Traditional GSM	92,188	4,030	0.201	0.8496	0.7729
Macroelement	215,200	12,118	0.182	0.0556	0.0695

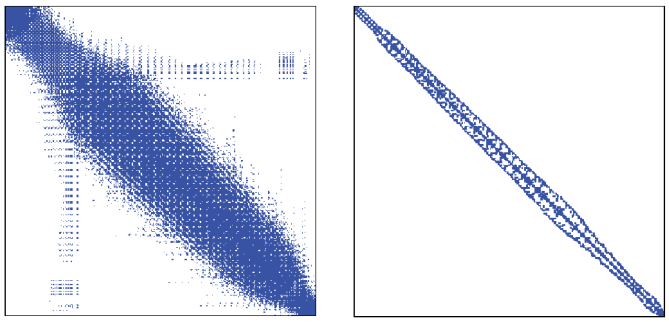

Fig. 11. Global stiffness matrix after applying the reverse Cuthill–McKee algorithm for the wrench example using: (a) traditional full-level GSM; (b) GSM with macroelement approach

approach is used, as given in Table 2. A greater sparseness in the stiffness matrix is seen in the macroelement approach, as shown in the visual comparison of the global stiffness matrices provided in Fig. 11. The reduction in the maximum semibandwidth and profile becomes increasingly significant, as the size of the stiffness matrix increases.

Applications to Structural Engineering Designs

Arch Bridge

An engineering application of the macroelement approach is examined using a bridge topology optimization as an example. Fig. 12(a) shows a typical arch bridge design in real life. The 2D bridge domain in Fig. 12(b) has supports, a cantilever, and a nondesignable layer that represents the bridge deck. The nondesignable layer is implemented by a discrete two-node beam element for both the GSM and the continuum method. In an effort to obtain constructible structures, the authors use a relatively coarse grid to discretize the domain (10×10 for the macroelement approach and 20×10 for the traditional GSM; both methods use structured quadrilateral discretization), as shown in Fig. 12(c). Unstable nodes and floating bars are removed, then the final topologies are checked to ascertain that they are at equilibrium (instability of members is not verified). The final topology obtained from the GSM using the macroelement approach is compared with those obtained from the traditional GSM and density-based optimization using PolyTop (Talischi et al. 2012b), as shown in Figs. 13(b–d). The numerical information is provided in Table 3.

The macroelement approach offers a solution that resembles a typical arch bridge shown in Fig. 13(a). When a coarse grid is used, the overall result of the GSM using the macroelement approach is improved in terms of constructability, because this approach is capable of generating various shapes of paths, thus providing clear layouts. In the comparison with other types of optimization methods, the GSM with the macroelement approach using a similar number of bars as the traditional GSM, not only gives a clear overall layout and provides a smooth arc top and fan feature on the topology, but also has a smaller compliance value. The traditional GSM, however, gives a topology with multiple layers along the top. The reason could be directions of paths are limited in the traditional GSM, thus, there are multiple force paths on the topology. When comparing results from the macroelement approach with the continuum optimization solution

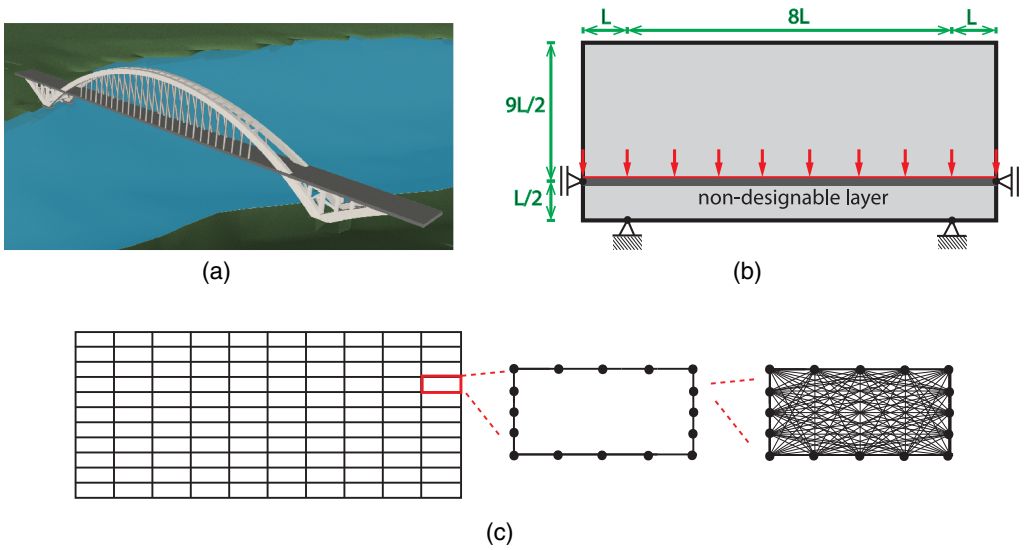

Fig. 12. Structural design for arch bridge example: (a) rendering of a typical arch bridge; (b) domain and boundary conditions; (c) discretization using macroelement approach with 10×10 grid and three inserted nodes per edge

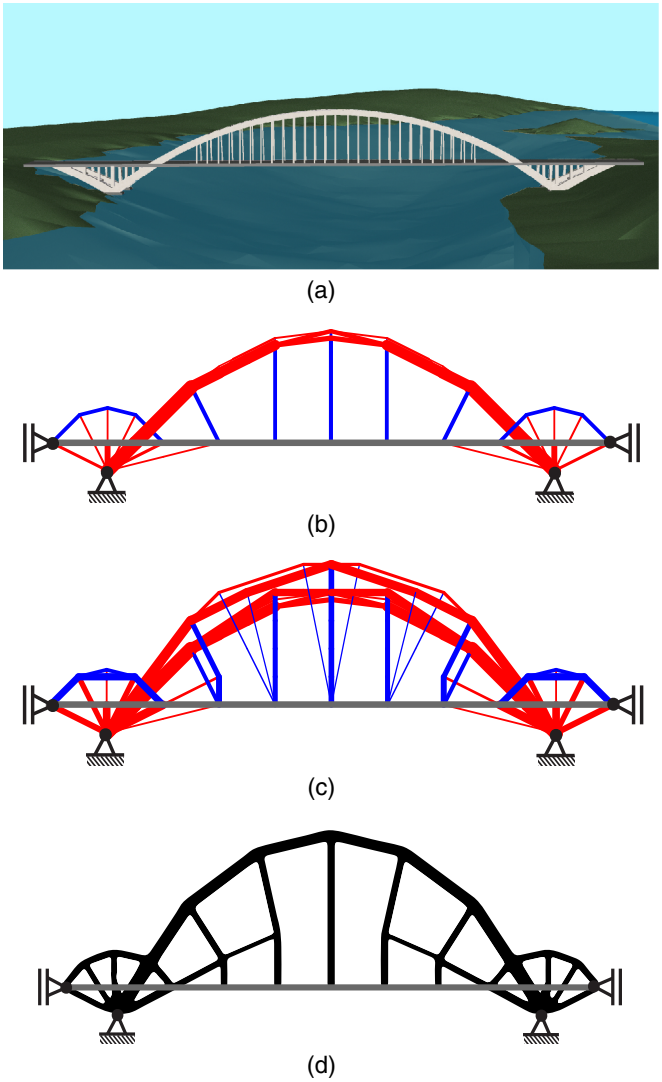

Fig. 13. Final topologies for arch bridge example: (a) rendering of a typical arch bridge; (b) truss optimization using the GSM with the macroelement approach (100 structural quadrilateral elements with three additional nodes inserted per edge); (c) truss optimization using the traditional GSM (200 structural quadrilateral elements); (d) continuum optimization using the density-based method ($R = 1.5$, volume fraction $= 0.15$)

Table 3. Numerical Information for Arch Bridge Example

GSM	Number of bars	DOFs	Compliance	$\lvert K_{\text{top}} u_{\text{top}} - F_{\text{top}} \rvert / \lvert F_{\text{top}} \rvert$
Traditional GSM	10,078	462	7.59	1.163×10^{-11}
Macroelement	8,840	1,562	7.18	2.149×10^{-11}

(obtained using PolyTop), qualitatively, both topologies appear to converge to the same solution and have similar traits, such as arc top and fan features on the left and right-hand-side of the topology. Furthermore, the macroelement approach provides vertical members on the topology, which is closer to the real-life design of an arch bridge. This suggests that the GSM using the macroelement approach offers promising and constructible structural designs.

Skyscraper Design: Lotte Tower

The conceptual design of a diagonal grid (diagrid) structure is illustrated in Figs. 14(a and b), which shows a square base transitioning to a circle at the top. This example is based on the design of the Lotte Tower in Seoul, Korea, by Skidmore, Owings & Merrill LLP (SOM) architects. The design domain dimensions are $10 \times 10 \times 80$, with all members initialized with the unit area. The macropatch approach is used in this example. Fig. 15(a) shows the initial patches defined over the domain. The patches are further subdivided, and all internal nodes within the patch are connected to each other using bar elements as a full ground structure, as illustrated in Fig. 15(b). The extent of the subdivisions of a patch for internal connectivity is user-defined. The overlapping of bars is still an issue; they are removed from the problem before any optimization takes place.

Fig. 16 shows an analysis performed for wind loading in one direction with imposed symmetry; and Fig. 17 shows the results for the case with wind loading applied in both directions with imposed symmetry using multiple load cases. The resulting designs illustrate how the load flows in a naturally cascading pattern, leading to a diagrid structure. Diagrid structures are stiff and contribute to limiting the drift of tall buildings. In addition, the fundamental aspects of high-rise building behavior are evident: The columns decrease in size from the bottom of the building to the top. When the wind is applied symmetrically from one direction, the final pattern shows thicker members in the direction of the wind. In the direction normal to the wind loading, the members are relatively thin and act as a web member for the building. In the second case, when the applied wind load is symmetric in both directions, the optimized building is symmetric and displays a diagrid pattern on all sides. The initial structure does not need to be finely discretized, as it is not feasible, from a construction point of view, to have a larger number of small bars in the optimized solution.

Diagrid solutions are not only artistic but also quite practical in design and can easily achieve efficiency with the use of steel for construction (Moon et al. 2007). These solutions have been used widely in the design of some very unique buildings. In general, the high stiffness of diagrid structures, with or without the use of corner columns, not only make them very desirable but an attractive solution to architects. In the typical structural design process, several iterations are needed in the design process to get the optimum diagrid solution, which is very time-consuming and may not result in a global optimized structure. Using the macropatch approach, it is possible to limit the time in the design process and easily estimate the final optimized diagrid solution.

Discussion and Concluding Remarks

In this paper, the generation of ground structures for generic 2D and 3D domains is discussed and explored. Two types of discretization are used, standard structured quadrilateral discretizations and Voronoi-based discretizations, which offer alternative methods for grid generation. In addition, two approaches for ground structure generation have been presented in an effort to improve the solutions of the GSM, the macroelement approach and the macropatch approach, which are designed to avoid invalid connectivity in the ground structure. The proposed approaches are investigated and have been demonstrated to improve the process of initial generation of ground structures, reduce the bandwidth of the stiffness matrix in the optimization process, provide a finer control of the final topology, and reduce the number of overlapping bars. Three types of examples are studied in this paper: (1) benchmark example: Michell truss; (2) nonbox domain: wrench; and (3) structural engineering applications: long-span bridge, skyscraper.

(a) (b)

Fig. 14. Conceptual design of the Lotte Tower by SOM architects: (a) full view (SOM | © SEVENTH ART GROUP); (b) top detailed view (SOM | © Archimation)

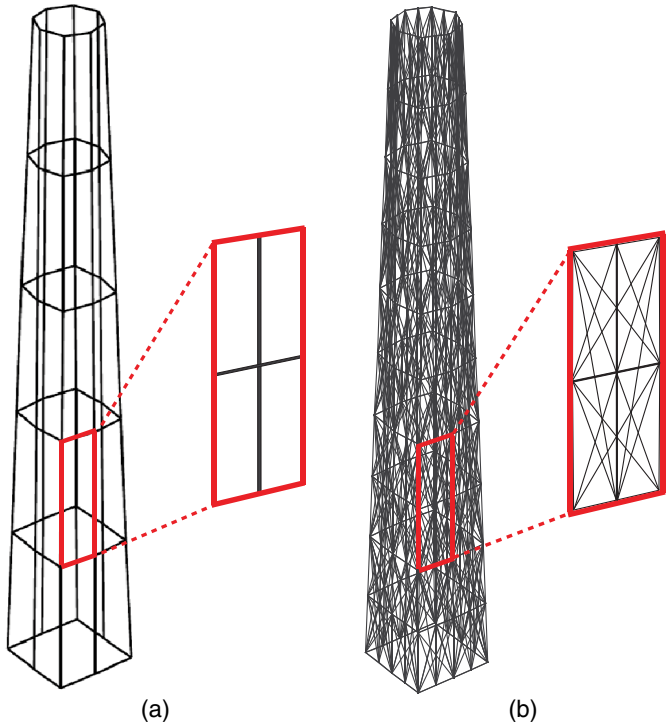

(a) (b)

Fig. 15. Lotte tower example using the macropatch approach with a structured quadrilateral surface grid: (a) initial patch definition of the design domain ($10 \times 10 \times 80$); (b) internal connectivity within the patches defined for the design domain

From the Michell truss example, the proposed macroelement approach yields similar discretized results to the analytical solution, and the curved features can be approximated by means of the proposed method. The wrench example highlights the capability of the

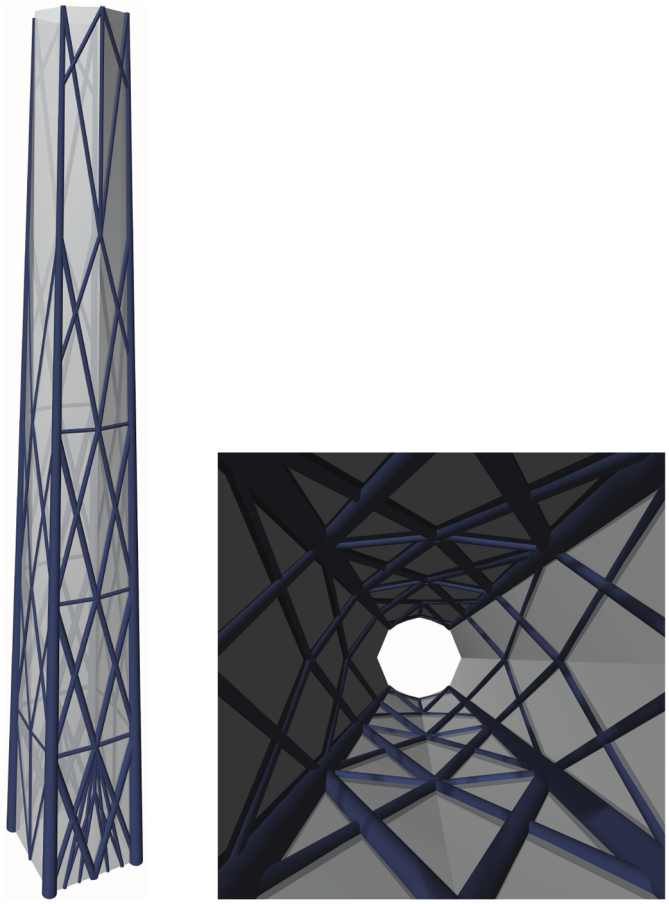

(a) (b)

Fig. 16. Final topologies for Lotte tower example using the macropatch approach with distributed wind load applied in a single direction with symmetry: (a) perspective view; (b) bottom-to-top view

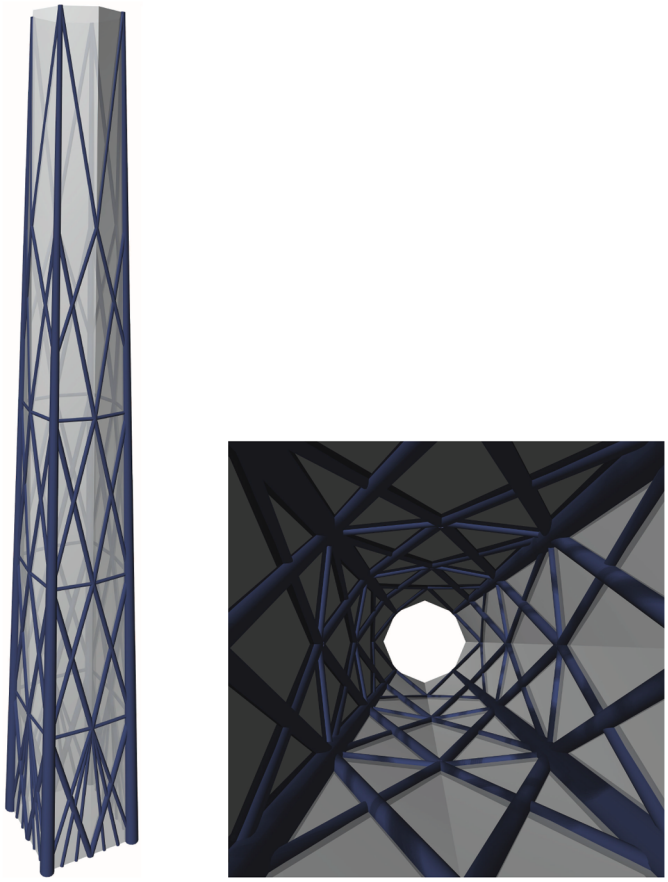

Fig. 17. Final topologies for Lotte tower example using the macropatch approach with distributed wind load applied in both directions with imposed symmetry: (a) perspective view; (b) bottom-to-top view

macroelement approach to handle large-size problems and nonbox (concave) domains. A greater sparseness is found in the stiffness matrix obtained from the macroelement approach, as shown in the investigation to verify the source of efficiency. In the bridge example, the macroelement approach leads to a solution that resembles a typical arch bridge (Fig. 13). The topology of GSM using the macroelement approach is improved in terms of constructability for coarse discretizations, because this approach is capable of generating various shapes of paths and thus provide clear layouts. In addition, final topology obtained from the macroelement approach shows agreement with that from the continuum structural optimization. The macropatch approach for the Lotte Tower leads to a diagrid-like structure, which is a typical design used in practice. This work offers room for future extensions, including exploring the macroelement for 3D Voronoi tessellations (Gain et al. 2014) and investigating the plastic formulation approach (Zegard and Paulino 2014, 2015).

Appendix. Optimality Criteria Method

The optimization in this work is solved by the OC algorithm. This algorithm can be derived by replacing the objective and constraints functions with the approximations on the current design point using an intermediate variable. In such a way, a sequence of separable and explicit subproblems is generated to approximate of the original problem. In this context, we linearized the objective function using exponential intermediate variables as (Groenwold and Etman 2008)

$$y_i = \left(\frac{a_i - a_i^{\min}}{a_i^{\max} - a_i^{\min}}\right)^{p_i} \tag{6}$$

$$C(\boldsymbol{a}) \cong \hat{C}(\boldsymbol{a}) = C[\boldsymbol{y}(\boldsymbol{a}^k)] + \left(\frac{\partial C}{\partial \boldsymbol{y}}\right)^{\mathbf{T}}_{a=a^k} [\boldsymbol{y}(\boldsymbol{a}) - \boldsymbol{y}(\boldsymbol{a}^k)] \tag{7}$$

Then, after substitution of $(\partial C/\partial y_i)_{a=a_i^k} = [(\partial C/\partial a_j)(\partial a_j/\partial y_i)]_{a=a_i^k}$ and substitution of Eq. (6) in Eq. (7), the following equations are obtained:

$$\hat{C}(\boldsymbol{a}) = C[\boldsymbol{y}(\boldsymbol{a}^k)] + \sum_{i=1}^{n} \left.\frac{\partial C}{\partial a_i}\right|_{a=a^k} \frac{1}{p_i}(a_i^k - a_i^{\min})\left[\left(\frac{a_i - a_i^{\min}}{a_i^k - a_i^{\min}}\right)^{p_i} - 1\right] \tag{8}$$

$$\min_{\boldsymbol{a}} \hat{C}(\boldsymbol{a}) \qquad \text{s.t.} \begin{cases} g(\boldsymbol{a}) = \boldsymbol{a}^{\mathbf{T}}\mathbf{L} - V_{\max} = 0 \\ a_{\min} \le a_i \le a_{\max} \quad \forall\ i = 1{:}M \end{cases} \tag{9}$$

By means of the Lagrangian duality, this problem can be solved with

$$L(\boldsymbol{a}, \gamma) = \hat{C}(\boldsymbol{a}) + \phi g(\boldsymbol{a}) \tag{10}$$

where ϕ = Lagrange multiplier, and the optimality conditions are given as

$$\frac{\partial L}{\partial a_i}(\boldsymbol{a}, \phi) = \frac{\partial \hat{C}(\boldsymbol{a})}{\partial a_i} + \phi \frac{\partial g(\boldsymbol{a})}{\partial a_i} = \left.\frac{\partial C}{\partial a_i}\right|_{a=a^k} \left(\frac{a_i - a_i^{\min}}{a_i^k - a_i^{\min}}\right)^{p_i - 1} + \phi L_i = 0 \tag{11}$$

$$\frac{\partial L}{\partial \phi} = \boldsymbol{a}^T \mathbf{L} - V_{\max} = 0 \tag{12}$$

Solving Eq. (11) for $a_i(\phi)$ to obtain

$$a_i(\phi) = a_i^* = a_i^{\min} + [B_i(\phi)]^{1/1-p_i}(a_i^k - a_i^{\min}) \tag{13}$$

and substituting in Eq. (12), the Lagrange multiplier ϕ is obtained, for example, using the bisection method in which B_i is defined as

$$B_i = -\frac{\left.\frac{\partial C}{\partial a_i}\right|_{a=a^k}}{\phi L_i} \tag{14}$$

To calculate ϕ and a_i^*, the box constraints need to be satisfied, and thus the next design point a_i^{new} is defined as

$$a_i^{\text{new}} = \begin{cases} a_i^+, & a_i^* \ge a_i^+ \\ a_i^-, & a_i^* \ge a_i^- \\ a_i^*, & \text{otherwise} \end{cases} \tag{15}$$

where the a_i^+ and a_i^- = bounds for the search region defined by

$$a_i^- = \max(a_i^{\min}, a_i^k - \text{move}) \tag{16}$$

$$a_i^+ = \min(a_i^{\max}, a_i^k + \text{move}) \tag{17}$$

in which the variable move is the move limit usually specified as a fraction of $a_i^{\max} - a_i^{\min}$. In the convex examples, presented in this work, a fast convergence is obtained using values for move larger than $a_i^{\max} - a_i^{\min}$.

The quantity $\eta = 1/1 - p_i$ is usually called a numerical damping factor, and for $p_i = -1$, a reciprocal approximation is obtained. The p_i values can be estimated using different approaches. In this

work, a two-point approximation approach is used based on the work of Fadel et al. (1990) and presented by Groenwold and Etman (2008). In this approach, the estimation of $p_i^{(k)}$ is

$$p_i^{(k)} = 1 + \frac{\ln\left(\frac{\partial C}{\partial a_i}\Big|_{a=a^{k-1}} \Big/ \frac{\partial C}{\partial a_i}\Big|_{a=a^k}\right)}{\ln(a_i^{k-1}/a_i^k)} \tag{18}$$

where $\ln(\bullet)$ = natural logarithm. In the first step $p_i = -1$ is used and $-15 \le p_i \le -0.1$ is restricted for the subsequent iterations. The convergence criteria used is

$$\max\left(\frac{|a_i^k - a_i^{k-1}|}{1 + a_i^{k-1}}\right) \le \text{tol} \tag{19}$$

where tol = tolerance.

Acknowledgments

The authors are grateful for the support from the U.S. National Science Foundation under Grant Nos. 1321661 and 1335160. They acknowledge the support from SOM (Skidmore, Owings and Merrill LLP), and from the Donald B. and Elizabeth M. Willett endowment at the University of Illinois at Urbana-Champaign. The authors also wish to extend their appreciation to Neil Katz for his help with this publication. Any opinions, findings, conclusions, or recommendations expressed in this paper are those of the authors and do not necessarily reflect the views of the sponsors.

References

Achtziger, W., and Stolpe, M. (2007). "Truss topology optimization with discrete design variables—Guaranteed global optimality and benchmark examples." *Struct. Multidiscip. Optim.*, 34(1), 1–20.

Bendsøe, M. P., Ben-Tal, A., and Zowe, J. (1994). "Optimization methods for truss geometry and topology design." *Struct. Optim.*, 7(3), 141–159.

Bendsøe, M. P., and Sigmund, O. (2003). *Topology optimization: Theory, methods, and applications*, Springer, Berlin.

Ben-Tal, A., and Bendsøe, M. P. (1993). "A new method for optimal truss topology design." *SIAM J. Optim.*, 3(2), 322–358.

Christensen, P. W., and Klarbring, A. (2008). *An introduction to structural optimization*, Vol. 153, Springer Science & Business Media, Dordrecht, Netherlands.

Cook, R. D., Malkus, D. S., Plesha, M. E., and Witt, R. J. (2002). *Concepts and applications of finite element analysis*, Wiley, Hoboken, NJ.

Cuthill, E., and McKee, J. (1969). "Reducing the bandwidth of sparse symmetric matrices." *Proc., 24th National Conf. of the ACM (Association for Computing Machinery)*, ACM, New York, 157–172.

Dorn, W. S., Gomory, R. E., and Greenberg, H. J. (1964). "Automatic design of optimal structures." *J. de Mecanique*, 3(1), 25–52.

Fadel, G. M., Riley, M. F., and Barthelemy, J. M. (1990). "Two point exponential approximation method for structural optimization." *Struct. Optim.*, 2(2), 117–124.

Gain, A. L., Talischi, C., and Paulino, G. (2014). "On the virtual element method for three-dimensional linear elasticity problems on arbitrary polyhedral meshes." *Comput. Methods Appl. Mech. Eng.*, 282, 132–160.

Gilbert, M., and Tyas, A. (2003). "Layout optimization of large-scale pin-jointed frames." *Eng. Computations*, 20(8), 1044–1064.

Groenwold, A. A., and Etman, L. (2008). "On the equivalence of optimality criterion and sequential approximate optimization methods in the classical topology layout problem." *Int. J. Numer. Methods Eng.*, 73(3), 297–316.

Hagishita, T., and Ohsaki, M. (2009). "Topology optimization of trusses by growing ground structure method." *Struct. Multidiscip. Optim.*, 37(4), 377–393.

Heath, M. T. (1997). *Scientific computing: An introductory survey*, 2nd Ed., Vol. 363, McGraw-Hill, New York.

Kirsch, U. (1989). "Optimal topologies of structures." *Appl. Mech. Rev.*, 42(8), 223–239.

Martinez, P., Marti, P., and Querin, O. (2007). "Growth method for size, topology, and geometry optimization of truss structures." *Struct. Multidiscip. Optim.*, 33(1), 13–26.

MATLAB [Computer software]. MathWorks, Natick, MA.

McKeown, J. (1998). "Growing optimal pin-jointed frames." *Struct. Optim.*, 15(2), 92–100.

Michell, A. G. M. (1904). "The limits of economy of material in frame-structures." *Philos. Mag.*, 8(47), 589–597.

Moon, K. S., Connor, J. J., and Fernandez, J. E. (2007). "Diagrid structural systems for tall buildings: Characteristics and methodology for preliminary design." *Struct. Des. Tall Spec. Build.*, 16(2), 205–230.

Ohsaki, M. (2010). *Optimization of finite dimensional structures*, CRC Press, Boca Raton, FL.

Rule, W. K. (1994). "Automatic truss design by optimized growth." *J. Struct. Eng.*, 10.1061/(ASCE)0733-9445(1994)120:10(3063), 3063–3070.

Smith, O. (1998). "Generation of ground structures for 2D and 3D design domains." *Eng. Computations*, 15(4), 462–500.

Sokół, T. (2010). "A 99 line code for discretized Michell truss optimization written in Mathematica." *Struct. Multidiscip. Optim.*, 43(2), 181–190.

Sokół, T., and Rozvany, G. I. N. (2012). "New analytical benchmarks for topology optimization and their implications. Part I: Bi-symmetric trusses with two point loads between supports." *Struct. Multidiscip. Optim.*, 46(4), 477–486.

Svanberg, K. (1984). "On local and global minima in structural optimization." *New directions in optimum structural design*, E. Gallhager, R. H. Ragsdell, and O. C. Zienkiewicz, eds., Wiley, Chichester, U.K., 327–341.

Talischi, C., Paulino, G. H., and Le, C. H. (2009). "Honeycomb Wachspress finite elements for structural topology optimization." *Struct. Multidiscip. Optim.*, 37(6), 569–583.

Talischi, C., Paulino, G. H., Pereira, A., and Menezes, I. F. M. (2010). "Polygonal finite elements for topology optimization: A unifying paradigm." *Int. J. Numer. Methods Eng.*, 82(6), 671–698.

Talischi, C., Paulino, G. H., Pereira, A., and Menezes, I. F. M. (2012a). "PolyMesher: A general-purpose mesh generator for polygonal elements written in Matlab." *Struct. Multidiscip. Optim.*, 45(3), 309–328.

Talischi, C., Paulino, G. H., Pereira, A., and Menezes, I. F. M. (2012b). "PolyTop: A Matlab implementation of a general topology optimization framework using unstructured polygonal finite element meshes." *Struct. Multidiscip. Optim.*, 45(3), 329–357.

Zegard, T., and Paulino, G. H. (2014). "GRAND—Ground structure based topology optimization on arbitrary 2D domains using MATLAB." *Struct. Multidiscip. Optim.*, 50(5), 861–882.

Zegard, T., and Paulino, G. H. (2015). "GRAND3—Ground structure based topology optimization for arbitrary 3D domains using MATLAB." *J. Struct. Multidiscip. Optim.*, 52(6), 1161–1184.